3D Spreadsheet numerical model; Potential ($\nabla\phi$) and stream ($\Delta\psi$) functions

Rodrigo Grossi grossirm@hotmail.com CEPAS|USP; Dário Vaz dariofvaz@hotmail.com GAC, SENAC - SP - BRAZIL

ARTICLE INFO

Keywords:

Potential functions

Stream functions

Relaxation method

Nodal equation

Spreadsheet

Flow field

ABSTRACT

The task of building of a functional groundwater flow model on a spreadsheet has become a traditional exercise in many hydrogeology classes around the world. From the seminal paper of Theo Olsthoorn (1985), the drawing of potential functions ($\nabla\phi$) are easily implemented by simple iterative numerical calculations, which makes use of the eventual annoying "circular reference error" of some standard application. The associated stream functions ($\Delta\psi$) approach is an alternative to be used, but difficulties emerge if attempts are made to have these two solutions at once. In this paper an expedite method is proposed to have a quick grasp of the interaction between potential and stream functions. The relaxation method was described, and a theoretical example tests the projections within a plausible a geological scenario.

Introduction

A spreadsheet is a friendlier interface when in comparison with any other modelling code. It avoids the shortcomings of not know the programming technicalities that would discourage an average would be modeller. Moreover, the possibility to build one's own groundwater flow model has not only the prospect of unveiling key aspects of the modelling procedures; this task also provides the user with insights about the meaning of all the outputs produced, as he gradually becomes the solely responsible for every single equation applied.

The intrinsically suited row-column structure of an electronic spreadsheet, coupled with the well-known Laplacian potential functions ($\nabla\phi$), has the power to display hydrogeology problems by the drawing of potentiometric maps. Bear (1972) strengthen its accuracy by the related stream functions ($\Delta\psi$), which works better indeed, if these two components are design to act together as a unified flow field. Further, updates softened the needed mathematical manoeuvres (Frind & Matanga, 1985; Foog et. al. 1985; Andreson & Woessner, 1995). But, besides being easily comprehensible when adopted separately, these methods require a complex reasoning if both gradients and streamlines are put together to interplay. I. e. the boundary conditions are not the same.

This article begins by collecting implicit assumptions scattered out on other theoretical papers, intending to clarify the building process of a flow field dual problem. Then an expeditious strategy to grasp the directions the flow lines ($\Delta\psi$) based on the hydraulic head field, or the potential function counterpart ($\nabla\phi$), is given by a strictly trigonometric standpoint.

Bibliographical revision

The motion of a fluid through the empty spaces of a porous media, by a mass conservation standpoint, is represented on the amount water (density ρw ≅ 1) stored in a cube of elementary volume (Figure 1).

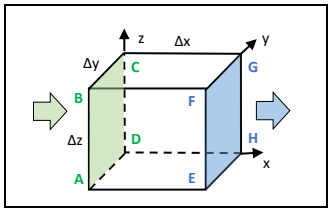

$$M_{EFGH} - M_{ABCD} = \frac{\partial\,(q_x)\Delta x\Delta y\Delta z}{\partial x} \qquad \textbf{Eq.1}$$

Fig. 1: (Domenico & Schwartz, 1990)

The INs and OUTs for the three cartesian directions gives the mass stored on a time basis (Equation 2):

$$\left(\frac{\partial q_x}{\partial x}+\frac{\partial q_y}{\partial y}+\frac{\partial q_z}{\partial z}\right) = -\frac{\partial(M_{x,y,z})}{\partial t} \qquad \textbf{Eq.2}$$

From the Darcy specific discharge ($QA = q = K\,[\partial_h/\partial_x]$), the potential functions ($\nabla\phi$), or hydraulic gradient, becomes a second derivative term (Equation 3):

$$KA\left(\frac{\partial[\partial_h/\partial_x]}{\partial x}+\frac{\partial[\partial_h/\partial_y]}{\partial y}+\frac{\partial[\partial_h/\partial_z]}{\partial z}\right) = 0 \qquad \textbf{Eq.3}$$

External components as an intake rate (Q); a seepage (P) per cross section area (A), plus the transmissivity (T) term (thickness [b] and hydraulic conductivity K) of the aquifer / layer analysed, gives the Laplace's continuous function for a stead state scenario (Equation 4):

$$Tx\frac{\partial^2 h}{\partial x^2}+Ty\frac{\partial^2 h}{\partial y^2}+Tz\frac{\partial^2 h}{\partial z^2} = Q + PA \qquad \textbf{Eq.4}$$

For transient outcomes (out of interest at moment) if a new constant (Ss) is provided, these equations include the release or storage of water for a correspondent hydraulic head change (Equation 5).

$$-\frac{\partial^2 h}{\partial x^2}+\frac{\partial^2 h}{\partial y^2}+\frac{\partial^2 h}{\partial z^2} = \frac{S_s}{K}\frac{\partial^2 h}{\partial_t} \qquad \textbf{Eq.5}$$

From the differential formulations to the nodal approach, the relaxation method bears the iterative process of numerical approximations, where each new step tries to diminish the difference between the gradients (hydraulic heads) of every two adjoining sides within a par of elementary volumes (Figure 2).

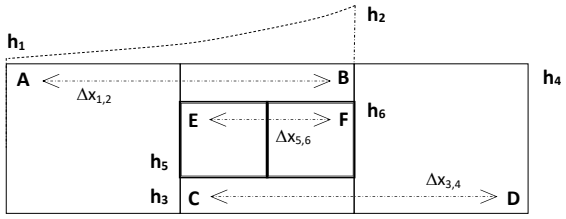

Fig.2: Nodal equation (Wang & Anderson, 1982; Poeter, 2008).

The block centred mesh of finite difference method Olsthoorn (1998) downscales the maths of the whole previously defined aquifer domain (Equation 6):

$$\frac{\partial^2 h}{\partial x^2}(EF) \cong \frac{[(\Delta h_{1,2})/\Delta x_{1,2}]-[(\Delta h_{3,4})/\Delta x_{3,4}]}{\Delta x_{5,6}} \qquad \textbf{Eq.6}$$

From the (x-y) bidimensional to the 3D point of view, comes the nodal continual form (Equation 7).

$$h_{i,j} = \frac{(h_N + h_S + h_E + h_W + h_T + h_B)}{6} - \frac{Q + PA}{6T} \qquad \textbf{Eq.7}$$

N, S, E, W, T, B: reference of north, south, east, west, top end bottom 3D neighbourhood cells

Then to eventually perform a 10% anisotropy feat, in a harmonic mean interpretation of the earlier mathematical definition (Poeter, 2008), Equation 8 is readily available for the spreadsheet.

$$h_{i,j} = \frac{(4T_H h_H + 0.1 * 2T_V h_V) + Q + PA}{4T_H h_H + 0.1 * 2T_V h_V} \qquad \textbf{Eq.8}$$

H and V: horizontal and vertical directions

Observations:

- In MS Excel, set maximum number of iterations ≈ 1000 for high loop limit value of circular references; set also maximum number of changes: ≈ 10^{-3}, the pace of convergence establishment;
- Codes such as USGS Modflow circumvent the Equation 8, in problems too big to process directly.

Modelling conceptions and constraints

Following a given geological situation, "fixed values" takes place as boundary conditions to restrain the performance of a modelled domain within acceptable margins of plausibility.

No flow (Dirichlet $\partial h/\partial L = 0$) potentiometric surfaces are a good example to start with (Figure 3):

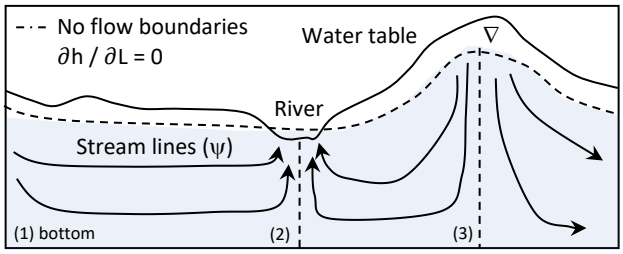

Fig.3: Regional water flow conceptual model

Figure 3 illustrate three of these boundary conditions:

1. A bottom horizontal impermeable bedrock layer;
2. A valley-floor divide a t the river thalweg;
3. And a ridgeline splitting two neighboring drainage basins (see leftside waters interactions in Figure 5).

Additionally, the Neumann type boundary conditions (not represented) can represent volumetric fluxes, in or outtakes as river infiltrations and pumping wells.

Application

A 3D numerical model was design to mimic a local *versus* regional theorical groundwater flow situation. Each 11 x 11 (rows x columns) x 5-layer (= 605) block-diagram node receives the same Equation 8 (Figure 4).

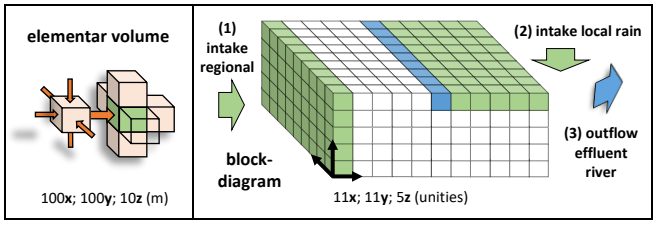

Fig.4: Node / elementary volume; intake / discharge areas;

Figure 4 also emphasize the water intakes (PA 1, QA 2) against a unique eleven blocks discharge area, the effluent river (3) up above halfway the model surface.

Table 1 describes the dimensions of the inflow areas.

Table 1: Inflow area dimensions e volumes (see Figure 4)

(→) Horizontal inflow (y, z)	**(↓) Vertical inflow (x, y)**
11 x 5 nodes of 100 x 10 (m) 0.055 Km² **of a transect area**	11 rows x 5 col. of 100 x 100 (m) 0.55 Km² **of seepage area**
Counterbalance input: regional volume search at Table 3	Input 1: q_{rain} = 300 (mm / year) of specific intake (flux / rains)

Numerical Results

Table 2 shows the 10th y mound pile cross section.

Table 2: Cross-section of the 10th y-row in table form

	1	2	3	4	5		1	2	3	4	5
1	14.8	14.8	14.7	14.6	14.6	14.6	14.7	14.9	14.9	15.0	15.0
2	14.8	14.8	14.7	14.6	14.6	14.6	14.7	14.8	14.8	14.9	14.9
3	14.8	14.8	14.7	14.6	14.6	14.6	14.7	14.7	14.8	14.8	14.8
4	14.8	14.8	14.7	14.6	14.6	14.6	14.7	14.7	14.7	14.8	14.8
5	14.8	14.8	14.7	14.6	14.6	14.6	14.7	14.7	14.7	14.7	14.8

These potentials ($\nabla\phi$) is seen with the derived stream vectors ($\Delta\psi$ arrows Figure 5). Records in annex.

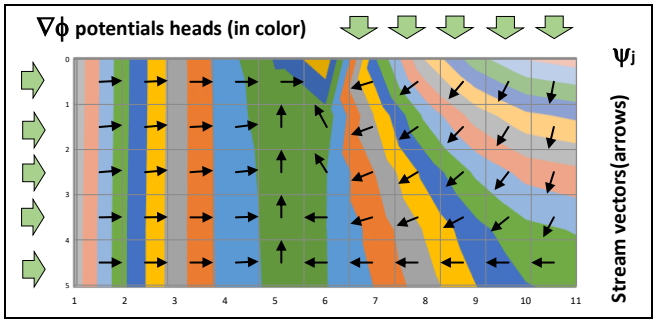

Fig 5: Cross-section of the 10th y-row in graphic form

Discussions

As a process of parameter optimization, a model calibration compares dependent and independent variables (soft x field data) (Olsthoorn, 1998), giving the modeller the opportunity to change any parameter required, to have the premises working accordingly with what is conceptually expected.

Three topics attest the plausibility of the present case model: 1) A analytical comparison of the disposed flow budget; 2) A visual analysis of the flow field produced; 3) And a cross-reference with real word recharge rates.

1) Figure 6 situates the physical locations of two cross-sections analytical darcyan comparisons: Horizontal and vertical volumes (X_{15}-X_{55}) x (Y_{17}-Y_{21}):

11	12	13	14	**15**	16	**17**	**18**	**19**	**20**	**21**
21	22	23	24	25	26	27	28	29	30	31
31	32	33	34	35	36	37	38	39	40	41
41	42	43	44	45	46	47	48	49	50	51
51	52	53	54	**55**	56	57	58	59	60	61

Fig. 6: Node locations at Table 2: 10th y-row (cross-section)

Table 3: Analytical view of numerical (Figure 6) chosen nodes

Regional outflow (→)	**(↓) Local intake**	
Gradients		
$i_V = \frac{(h_{15} - h_{55})}{(L_{15} - L_{55})} = 0.043\%$	$i_H = \frac{(h_{17} - h_{21})}{(L_{17} - L_{21})} = 0.043\%$	
Kv* = 0.10Kh **(vertical anizotropic hydraulic conductivity)**		
Kv = 15.77 (m/y) q_v= (Kv* i_v) = 0.068 (m/year)	Input 2 Kh = 157.68 (m/y) qh = 0.0068 (m/year)	
To the cross sections areas of Table 1		
Qv = qv * 55,000 m^2 Qv = 3,714 (m^3/year)	Qh= qh * 550,000 m^2 Qh = 3,719 (m^3/year)	Resídual error 1%
Input 3: 10% of direct aerial seepage (of q_{rain} Table 1); Input 4: river front 11th node: 15m plus 1% declivity (fixed head)		
Input 5: Horizontal (regional) flux intake 9.13 times the vertical (local) one to balance the model with littre residuals (Qx ≅ Qy)		
This balance results in 7,433 (m^3/year) of river total outflow, respecting 6.5 % of especific porosity and 95% of filled void space (see MS Excel solution spreadsheet)		

2) Figure 5 shows the achievement of the compulsory perpendicularity between potential and stream functions (Freeze & Cherry, 1979), mimicking a theoretical regional x local aquifer behaviour (details on drawing the flow paths in annex).

- The equipotential's (spaced curved colours of Figure 5) displace the flow velocities.

- Interestingly, at least for a layman, the left and right waters do not intermingle below the river.

- The elegant analytical sinusoid formulas of József Tóth (1962) first demonstrates such phenomenon, numerically updated on a not less outstanding manner by Molano (2013).

- Apropos, against Franklin Hiram King back in 1899, Hubbert (1940) first stablished the mass conservation principle for the groundwater flow.

From King's initial argument (Figure 7a), Hubbert demonstrates that the amount of energy per mass unit to transport the water from one to another equipotential surface must be the same. This being the cause that maintains apart the flow lines within a flowtube (Figure 7b); those convergence would be possible only in recharge and discharge regions.

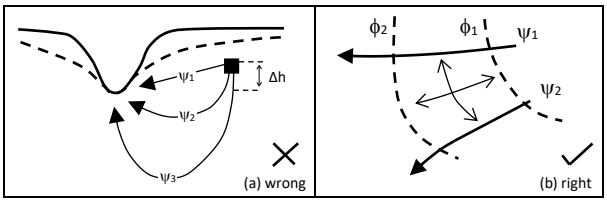

Fig. 7: Flow field of (a) King (1899) and (b) Hubbert (1940)

3) Returning to the raised numerical model report, the recharge and discharge areas must follow a typical theoretical volumetric proportion.

- Early conjectures on the genesis the aquifer waters empowered the hypothesis for the meteoric origin of the broad majority of ground waters. Table 4 shows the ratios between available recharge area and its discharge in a river (Meinzer, 1942. Apud Custodio & Llamas, 1996, p. 1102).

Table 4: Analytical x Numerical results comparison

Recharge Area	**Discharge Vol.**	**Font**
01 (km^2) ± 1‰	Q = 1 (l/s)	Custodio *et al.*
0.55 (km^2)	Q = 1.6 (l/s)	3D model

On average, the expected ratios of the literature revision are in order with the values of the present 3D model, considering the documented uncertainty.

The spreadsheet of this solution is currently [December, 2021] available at:

https://drive.google.com/file/d/149-KzSx4AJ0XzZMfu1NqrTw_R4-Q20Pt/view?usp=sharing

Annex

Although the lack of accuracy, a quick grasp of the flow field ($\Delta\psi$) can be achieved by an array of vectors derived from the potential lines passing by.

First, each hydraulic head was associated with its respective cardinal direction. Then by trigonometry a consequent angle is defined (Equation 9):

$$\theta = \frac{360\Delta h_{x(\rightarrow)} + 180\Delta h_{x(\leftarrow)} + 270\Delta h_{y(\downarrow)} + 90\Delta h_{y(\uparrow)}}{\Delta h_{x(\rightarrow)} + \Delta h_{x(\leftarrow)} + \Delta h_{y(\downarrow)} + \Delta h_{y(\uparrow)}} \quad \textbf{Eq.9}$$

$360_{(\rightarrow)}\ 180_{(\leftarrow)}\ 270_{(\uparrow)}\ 90_{(\downarrow)}$ adopted as directions guides

Example (Figure 8): From the potential functions ($\nabla\phi$), i.e. from the calculated hydraulic heads, only those positive differences was taken in account to find the nodes stream vectors.

H	1	2	3	...
1	1.95	2.09	2.42	
2	1.93	1.99	2.11	
3	1.89	1.86	1.78	
...				

V	1	2	3	...
1	0.00	0.00	0.00	
2	0.06	0.09	0.19	
3	0.10	0.13	0.27	
...				

$$\theta_{22} = \frac{(360*1.99)+(180*0)+(270*0.09)+(90*0)}{1.99_{(\rightarrow)}+0_{(\leftarrow)}+0.09_{(\downarrow)}+0_{(\uparrow)}} = 356º$$

Fig. 8 Stream vector $\theta_{2,2}$ from horizontal / vertical H. differences

Other adopted defaults:

- Each vector's starting position was settled in the middle of the respective block-diagram node;
- A half unity length (0.5) was predefined as the length of all flow vectors. They act like a hidden hypotenuse between the adjacent and opposed cathetus / nodes.

Once defined the start point and the node angle, the vector end point comes from Pythagoras's theorem (Figure 9):

Vector ψ_{22} definition, from predefined start position and angle (with MS Excel degree to radian conversion)	
$x_2 = x_1 + (\cos\theta)/2$ $y_2 = y_1 + (\mathrm{sen}\theta)/2$ $\theta_{rad} = (\theta°) * (\pi/180)$	**Start point (X_1, Y_1) A (1.5, 1.50)** End point (X_2, Y_2) B (2.0; 1.47)

Fig. 9 Stream vector Equations and result at cell $_{2,2}$

Bibliography

Andreson, M. P., Woessner, W. W. 1995 Applied Groundwater Modeling: Simulation of Flow and Advective Transport – First Edition, 381 pag., Academic Press – Elsevier.

Bear, J. 1972 Dynamics of Fluids in Porous Media, American Elsevier Publishing Co., NY, pp. 687-701.

Custodio, E., Llamas, R.M. 1996 Hidrología Subterránea - Omega, S.A., Ediciones.

Domenico, P.A., Schwartz, F.W. 1990 Physical and chemical hydrogeology, 849p. Texas A&M University – Jobn Winey and Sons.

Foog G. E., Senger R, K. 1985 Automatic Generation of flow Nets with Conventional Ground-water Modeling Algorithms Ground Water, vol 23, no 3, pp 336-344

Freeze R. A., Cherry J. A. 1979 Groundwater, Prentice-Hall, Universidade de Michigan, 604p.

Frind E. O., Matanga G. B. 1985 The dual formation of flow for contaminant transport modelling, 1. Review of theory and accuracy aspects. Water Resources research. V. 21, no 2, pp 159-169

Hubbert, M.K. 1940 The theory of groundwater motion. The Journal of Geology

King, F.H. 1899 Principles and conditions of the movements of ground water. U.S. Geological Survey 19th Annual Report, Part 2.

Molano C. 2009 Groundwater Spreadsheets: A Simple Tool for Solving Efficiently Groundwater Flow and Pollution Analytical and Numerical Problems. https://www.youtube.com/watch?v=sD1BSQA2w7w

Olsthoorn T. N. 1985 The power of electronic worksheet modelling without special programs. Ground Water

Olsthoorn, T. N. 1998 Groundwater Modelling: Calibration and the Use of Spreadsheets.

Poeter P. E. 2008 Ground Water Modeling Course.

Tóth, J. 1962 A Theory of Groundwater Flow in Small Drainage Basins. Journal of geophysical search. Volume 65, No. 16.

Tóth, J. 2009 A brief history of the theory of gravity-driven regional groundwater flow.

Vaz, D. A., Grossi R. M. 2016 Emprego de planilhas eletrônicas padrão MS Excel para modelagem matemática de aquíferos por diferenças finitas Senac -SP, 40 f.: il. color.

Wang, H. F., Anderson M. P. 1982 Introduction to Groundwater Modeling: Finite Difference and Finite Element Methods. 246 pages - Academic Press. University of Wisconsin, Madison.